

# Controlling the Shape of Evaporating Droplets by Ionic Strength: Formation of Highly Anisometric Silica Supraparticles\*\*

Marcel Sperling, Orlin D. Velev,\* and Michael Gradzielski\*

**Abstract:** Anisometric silica supraparticles are produced by a simple process of evaporation of sessile droplets containing fumed silica deposited on a superhydrophobic substrate. The shape of the supraparticles is directly controlled by the salt (NaCl) concentration, becoming anisometric beyond a threshold concentration, as quantified by light microscopy. This process is easily extended to supraparticles containing further functional colloidal components.

The formation of macroscopic particles with mesoscopic substructuring has been the topic of many investigations in recent years.<sup>[1]</sup> One facile technique for synthesizing such supraparticles is the evaporation of colloid-particle-containing aqueous droplets on a superhydrophobic surface.<sup>[2]</sup> Such controlled self-assembly of colloids into coagulated or precipitated superstructures<sup>[3]</sup> in confined geometries (the evaporating drop) allows well-defined hierarchically structured supraparticles to be fabricated.<sup>[4]</sup> They are very interesting as new functional and smart materials,<sup>[1,5]</sup> and owing to their compositional and structural variability, supraparticles have potential for use in various applications, such as catalysis,<sup>[6]</sup> thermo- or magneto-sensitive materials,<sup>[7]</sup> lithography,<sup>[8]</sup> microfluidics,<sup>[9]</sup> or sensing.<sup>[10]</sup>

We employed the method of droplet templating by evaporation induced self-assembly (EISA) of a sessile droplet of a colloidal suspension deposited on a solid superhydrophobic substrate. The method of droplet templating was shown before to lead to symmetric supraparticles,<sup>[2]</sup> whereby often spherical, but also “doughnut” particles have been prepared,<sup>[11]</sup> taking advantage of the coffee-ring effect.<sup>[12]</sup> However, in general, shape control of supraparticles is not

easily achieved and obtaining anisometric particles with lower but controlled symmetry in a simple way has been a persistent challenge. Anisometric particles are very interesting for instance in dynamic flows, such as in the emerging area of self-propelling particles,<sup>[13]</sup> (note for example that real boats would never be built having a circular shape), or because of their ability to become oriented in external fields (shear, electric, or magnetic), or as demonstrated in a recent application of miniaturized stirring bars.<sup>[14]</sup> Accordingly shape control and formation of anisometric supraparticles by spontaneous, yet controlled, self-assembly is a problem of interest in colloid and material science.

Herein we present a novel approach for preparing highly anisometric supraparticles by a simple method using aqueous suspension droplets of fumed silica (FS) containing varying amounts of electrolyte, which are deposited on a superhydrophobic substrate and the solvent is allowed to evaporate at ambient conditions. The process of supraparticle formation during evaporation as a function of time was characterized by optical microscopy and an analysis of the final shape of the supraparticles after complete drying was performed.

The initial FS suspensions were prepared by dispersing FS in water, giving dilute suspensions (at higher concentrations the systems are too turbid for DLS experiments) in which polydisperse aggregates of approximately 150 nm radius (DLS; PDI = 0.2–0.4) are present (see Figure S1 and Table S1 in the Supporting Information) at pH 5.7. It should be noted that in FS the small primary particles form bigger aggregates as a result of incomplete sintering during the preparation process.<sup>[15]</sup> The NaCl concentration was adjusted to the desired value by mixing the FS stock suspension with an appropriate amount of aqueous NaCl solution and then diluting to a given concentration. For the preparation of the supraparticles, droplets of 3  $\mu$ L of these suspensions were deposited with a micropipette onto a superhydrophobic Cu–Ag substrate, which had been prepared by a procedure reported by Gu et al.<sup>[16]</sup> The droplets were then enclosed in a sealed glass chamber and allowed to dry at an average humidity of  $(43 \pm 10)\%$ , avoiding any air streams. After about 30–45 min, solid supraparticles resulted, which did not change any further, that is, the drying process was complete by then. Afterwards the dry particles lying on the superhydrophobic surface can easily be collected by slight tapping the surface.

This process was monitored by time-resolved microscopy and an example video for a sample with 5 mM NaCl (see video S2 in the Supporting Information) nicely illustrates how, for a long period, symmetric shrinking is observed and after some time, doughnut ring formation takes place. Then at a certain moment a sudden and anisometric deformation of the shrinking droplet occurs. The resulting anisometric

[\*] M. Sperling, Prof. Dr. M. Gradzielski  
Stranski Laboratorium für Physikalische und Theoretische Chemie  
Institut für Chemie, Technische Universität Berlin  
Strasse des 17. Juni 124, Sekr. TC7, 10623 Berlin (Germany)  
E-mail: michael.gradzielski@tu-berlin.de  
Homepage: <http://www.chemie.tu-berlin.de/gradzielski/>  
Prof. Dr. O. D. Velev  
Department of Chemical and Biological Engineering  
North Carolina State University (NCSU)  
911 Partners Way, Raleigh, NC 27695-7905, (USA)  
E-mail: odvelev@ncsu.edu

[\*\*] We are grateful for the financial support of this study from the Deutsche Forschungsgemeinschaft (DFG) in the framework of IGRTG-1524 and in the form of Mercator Professorship for O.V. (DFG INST131/582-1). We also acknowledge support from the US-NSF through the Triangle MRSEC on Programmable Soft Matter (DMR-1121107).



Supporting information for this article is available on the WWW under <http://dx.doi.org/10.1002/anie.201307401>.

structure, shaped like a boat, subsequently shrinks further without notably altering its shape during the final part of the drying process. Just before complete drying the supraparticle briefly turns very milky but the finally obtained fully dry particle is nearly transparent again. Another movie for low (0.1 mM) initial NaCl concentration illustrates a case where the spherical shape is retained during the entire drying process (Video S1).

We demonstrated that the specifics of this process and especially the resulting final structure of the supraparticles depend largely on the composition of the initial dispersion. The dry particles show slightly translucent appearance and a pronounced variation of shape, depending mainly on the initial ionic strength and to a much lesser extent on the FS content. Their shape and, in particular, their anisotropy were characterized by measuring the ratio of the lengths of long to short principal axes (Scheme S1). Representative examples of supraparticles obtained by variation of the initial FS and NaCl concentration are presented in Figure 1.

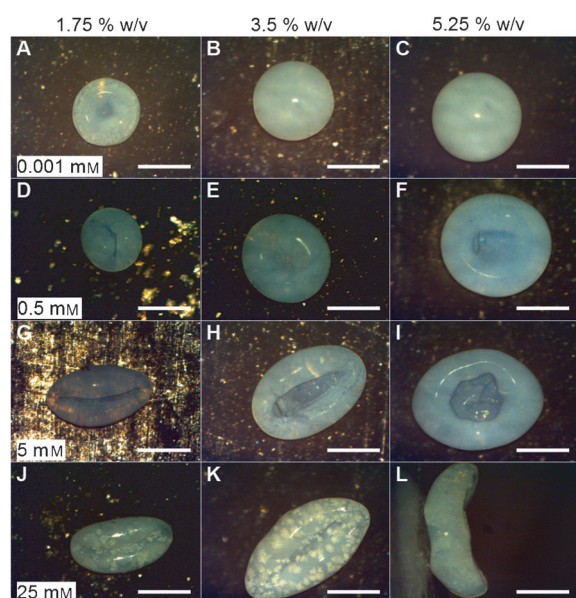


**Figure 1.** Examples of different types of supraparticles formed after completion of the drying process as a function of FS and electrolyte concentrations. From left to right the initial droplet concentrations are: 1.75, 3.5, 5.25 % w/v FS; From top to bottom: 0.001, 0.5, 5, 25 mM NaCl. The micrograph at bottom right shows side view of a folded “boat-like” structure. Scale bars: 0.5 mm.

Particles with rotational symmetry (spherical for high FS concentration and doughnut-shaped for lower FS concentration) are always obtained for very low NaCl concentrations of less than 0.5 mM (Figure 1 A–C), whereas for concentrations around 0.5 mM, the particles begin to show slight anisotropy (Figure 1 D–F). In contrast, even for 5 mM NaCl a much different behavior is evident and doughnut-like particles are observed for high initial FS content (Figure 1 I), which become increasingly anisometric for lower FS concentration (Figure 1 G,H), thereby resembling “boats”, that is, with

increasing the NaCl/FS ratio the structures are more elongated. The anisotropy of particle shape is most pronounced in droplets from solutions of 25 mM NaCl (Figure 1 J–L). In general, an increase of the FS concentration leads to larger particles and is accompanied by a transition to less anisometric particle shapes. In either case, the concentration of electrolyte is the predominant control parameter for the particle anisotropy, while the content of FS determines mainly the total particle volume.

The process of supraparticle formation was characterized comprehensively for different starting concentrations of FS and NaCl and the resulting anisotropy of the particles was analyzed in a quantitative manner by the ratio of the two principal axes of a rotational ellipsoid that can be fitted into the shapes of the final particles (for details see Figure S1). In Figure 2 we present the anisotropy data as a function of the

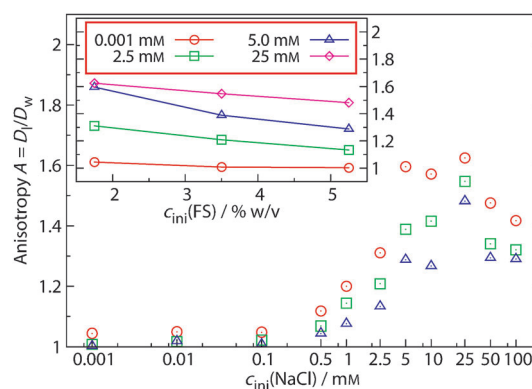


**Figure 2.** The degree of anisotropy of the dried FS supraparticles as a function of the initial NaCl concentration for three different initial amounts of FS: 5.25 (triangles), 3.50 (squares), and 1.75 % w/v (circles). Inset: dependence of the anisotropy on the FS concentration for four NaCl concentrations (average of 30 particles per data point).

initial NaCl concentration, obtained from analyzing the shape of 30 supraparticles after complete drying (note there is a substantial variance of the anisotropy of individual particles). Average anisotropy values of up to 1.6 are reached, rising linearly from 0.5 mM on a logarithmic concentration scale until a maximum anisotropy is achieved around 25 mM NaCl. For higher NaCl concentrations the degree of anisotropy remains unchanged or even becomes somewhat smaller. An initial concentration of approximately 0.5 mM NaCl is apparently the threshold value for achieving anisotropy, and depends only weakly on the FS concentration. The inset of Figure 2 shows that, for a given initial NaCl concentration, the anisotropy decreases somewhat with increasing FS concentration (see also Figure 1). However, this effect is much weaker than that of the ionic strength.

The ability to control the anisotropy by the salt concentration is an unexpected and interesting finding especially as even relatively low concentrations of NaCl in the mM range have very pronounced effects on the structural development of the drying supraparticles and the question arises by which mechanism this formation of anisometric particles proceeds. A sound hypothesis of the mechanism responsible for this

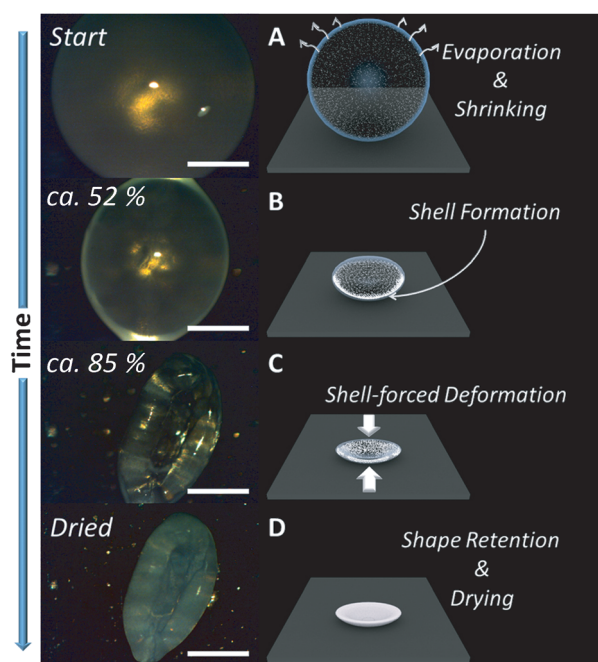


**Figure 3.** Microscopy images (left) from the drying process (initial concentrations: FS 3.5% w/v, 5 mM NaCl) with the percentage (of time) of the evaporation process until reaching the dry solid state. Scale bars: 0.5 mm. Schematic mechanism (right) of particle elongation during the evaporation process on a superhydrophobic Cu–Ag substrate.

shape transition, based on the temporal evolution of the droplets seen in the Videos (Supporting Information), is proposed in Figure 3. We consider four key steps (A–D), to explain the development of anisotropy during the evaporation process.

Initially the suspension droplet deposited onto the superhydrophobic substrate contains a homogeneous dispersion of ingredients (Figure 3A). During the evaporation of the liquid, the concentration of FS at the droplet's surface increases (Figure 3B). This increase occurs because as the droplet shrinks and the surface of the droplet moves nearer to the center of the droplet. This change is counterbalanced by FS and electrolyte diffusion. The rate  $\Delta r(t)$ , by which the surface front advances towards the center of the droplet can be evaluated by taking into account the droplet radius  $r(t)$  [Eq. (1)], with  $v_e$  being the velocity of droplet shrinkage owing to evaporation and  $r_0$  the initial droplet radius. This dependence on time has been measured (Figure S3) and  $v_e$  found to be  $0.17\text{--}0.28\ \mu\text{m s}^{-1}$ , depending on the humidity maintained in the chamber. This result must be compared to the movement resulting from diffusion. For the FS particles the diffusion coefficient  $\bar{D}_{\text{FS}}$  is  $1.45 \times 10^{-8}\ \text{cm}^2\text{s}^{-1}$  (DLS). Comparing the distance of the moving evaporation front [Eq. (1)] to the average diffusion path of the individual components [Eq. (2)], we find that after about 100 s the evaporation-caused surface propagation towards the interior becomes larger than the diffusion path of the FS particles (Figure S4) so that this diffusion can no longer balance out the effects of surface propagation. In contrast, the electrolyte

concentration profile remains homogeneous throughout the droplet as the salt ions, with  $\bar{D}_{\text{NaCl}}$  for NaCl being  $1.6 \times 10^{-5}\ \text{cm}^2\text{s}^{-1}$ ,<sup>[17]</sup> diffuse rapidly enough to avoid gradients during the evaporation time until the drying of the droplet is complete.

$$\Delta r(t) = r_0 - r(t) = -v_e(t) \quad (1)$$

$$\Delta x = \sqrt{2\bar{D}_{\text{FS/NaCl}}\Delta t} \quad (2)$$

From this estimate we conclude that FS particles will accumulate at the water–air interface and form an increasingly thick shell, whose structure and rigidity depends on the ionic strength, whereas the NaCl concentration profile remains homogeneous throughout the evaporating droplet. An increasing ionic strength decreases the electrostatic repulsion between the FS particles and therefore leads to a higher tendency for agglomeration and coagulation that affects the compactness and rigidity of the surface silica shell formed. This is also evidenced by the viscosity increase of FS solutions with increasing NaCl concentration (Figure S5). Apparently, above a critical concentration of NaCl of about 1 mM, (corresponding to a Debye screening length of ca. 10 nm) the shell becomes so rigid that upon further evaporation it can no longer flexibly adapt to an increasingly more curved spherical shape. Accordingly, a tension builds up (similarly to a deflating balloon with a stiff shell), which naturally leads to folding and an anisometric deformation of the shell (Figure 3C). At this point a breaking of the symmetry occurs, the symmetry for the “doughnut” is still relatively high ( $D_{\infty h}$ ), but that of the boat-shaped particles is much lower ( $C_{2v}$ ). This anisometric shape then is retained until complete drying to yield solid and collectable supraparticles (Figure 3D). The amount of NaCl contained is usually rather small (e.g. 1.7 wt% for a starting mixture of 3.5% w/v FS, 10 mM NaCl). Overall this translates into control of the shape of the supraparticles by the ionic strength of the drying solution. Of course, the details of this process also depend substantially on the humidity during the evaporation process. For high humidity the evaporation becomes so slow that no more shell formation occurs, while at much lower humidity it becomes so fast that only rather ill-defined particles are formed (Figure S6). Asymmetric deformations (“buckling”) have also been seen for drying polymer solutions,<sup>[18]</sup> but these are related to a much stronger pinning to the surface (contact angles below  $90^\circ$ ) and there are also theoretical descriptions of such buckling transitions.<sup>[18c]</sup>

In addition to the new uncommon shape, the FS supraparticles are remarkable for their optical appearance. Unlike earlier supraballs, made of arrays of diffractive, but highly scattering, polystyrene latex microspheres,<sup>[19]</sup> the close-packed nanometer-sized silica is optically translucent and homogeneous. The transparency of the FS supraparticles increases to a near completely transparent lens-like state when immersed in water (Figure 4A, owing to the similarity of the refractive indices), a change which is fully reversible (Figure 4B), which also demonstrates that these supraparticles have long-term stability (checked for more than 2 weeks) when dispersed in water or salt solution, a fact property from



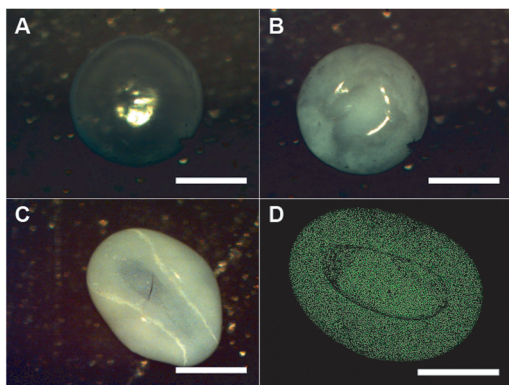


**Figure 4.** Variation of the optical appearance of the supraparticles. A) Nearly transparent supraparticle obtained by immersing the dry FS supraparticle in water. B) Sample shown in (A) after drying again. C) anisotropic particle with added latex (white patterns, 0.96  $\mu\text{m}$  PS latex microspheres). D) Analogous to (C) but with 1.077  $\mu\text{m}$  fluorescent yellow/green PS latex microspheres (Scale bars: 0.5 mm).

the irreversible aggregation of the FS aggregates during the drying process.

The properties of the FS supraparticles can be modified further by using the same generic process to assemble other colloidal components within the droplets, thereby yielding hybrid supraparticles. This principle was demonstrated by assembling mixed systems in which the initial suspension contained, in addition to the FS, other colloids as well. As an example, opaque boat-like structures were formed by adding polystyrene (PS) latexes. This is shown in Figure 4C for adding normal PS latexes of 0.96  $\mu\text{m}$  diameter and in Figure 4D for adding fluorescent PS latexes, where the fluorescence imparts additional functionality to the supraparticles, but it is clear that other colloids could easily be incorporated that would give interesting optical, electric, magnetic, or catalytic properties to the supraparticles, as the anisometric symmetry and shape is conducive to their alignment in external fields (for example, electric, magnetic, shear).

In summary, we present for the first time supraparticles based on fumed nanosilica (FS), an extremely versatile colloidal building block, available in large quantities. These FS nanoparticles can be assembled into highly anisometric supraparticles by means of a simple evaporation process on a superhydrophobic surface. The shape of the self-assembled particles can be controlled in a systematic fashion by varying the ionic strength of the FS-containing aqueous solution. Beyond a threshold ionic strength “boat-like” anisometric supraparticles are formed, which is a substantial extension to recent work dealing with the formation of radially symmetric “doughnuts” on superhydrophobic substrates.<sup>[11b]</sup> This asymmetric deformation mechanism consists of a first step similar to doughnut-ring formation and a second step involving anisometric shell deformation during further evaporation. This deformation is due to an evaporation-driven formation of a dense layer of agglomerated FS that becomes increasingly rigid with increasing NaCl concentration. Beyond a threshold concentration of about 1 mM NaCl, the silica layer becomes so stiff that it cannot follow an isometric reduction of volume any further and, like a deflating ball,

folds into an elongated structure. The degree of anisotropy depends on the concentration of NaCl, and to a much lesser extent on the FS content. The formation of anisometric supraparticles is a generic phenomenon, offering the possibility to incorporate additional components, such as latex microspheres or functional colloids such as magnetic, catalytic or optically active nanoparticles, into the supraparticles, and thereby combine these functional properties with the options offered by anisometric particles (such as their behavior in flow fields or anisotropic ordering). Therefore this facile process is an universally applicable tool for creating new types of anisometric and substructured colloidal particles, which could also be produced on larger scales, for example, by droplet ejection by inkjet-printing.<sup>[20]</sup> This class of novel supraparticles incorporating various colloids should have wide potential use in fields such as catalysis, microfluidics, sensing.

### Experimental Section

**Preparation of fumed silica stock suspension:** Solid fumed silica (FS; Sigma Aldrich: 7 nm primary particle, surface area =  $(395 \pm 25) \text{ m}^2 \text{ g}^{-1}$ ,  $\rho_{\text{bulk}}(25^\circ\text{C}) = 0.037 \text{ g mL}^{-1}$ ) was dispersed in miliQ-grade water under vigorous stirring for 3 h. The FS stock suspension was washed following a procedure reported by Velev et al.<sup>[11b]</sup> The suspension was centrifuged at 1600 g for 30 min, the supernatant solution was decanted, replaced with water, and the residue was redispersed by vortexing. After the third centrifugation the residue was redispersed in a small amount of water (ca. 1–2 mL), and sonicated for 45 min at room temperature. The final concentration was then adjusted to 0.07  $\text{g mL}^{-1}$  (i.e. 7% w/v) resulting in a viscous suspension of milky appearance, with pH 5.7 and an average particle agglomerate size of about 150 nm hydrodynamic radius with a PDI (polydispersity index) of about 0.3–0.4 (DLS: ALV/CGS-3 Compact Goniometer System,  $\lambda = 632.8 \text{ nm}$ ). DLS data are given in Figure S1 and Table S1. The polystyrene latex particles of 0.96 nm were obtained from Bangs-Labs and the fluorescent PS particles of 1.077  $\mu\text{m}$  were from Polysciences.

**Synthesis of the superhydrophobic surfaces:** The surface was prepared by an electrochemical deposition (ECD) process reported by Gu et al.<sup>[13]</sup> Polished copper plates were immersed into a slowly stirred solution of  $\text{AgNO}_3$  (10 mM) in water for 25 min at ambient temperature. Afterwards the blackish plates were gently washed with water and immersed into a solution containing dodecanethiol (1 mM) in ethanol for 20 h at ambient temperature. The resulting plates were washed with ethanol and water and the water contact angle was determined to be at 160–170° with a contact angle system instrument (DataPhysics OCA15plus). The contact angle was constant over several weeks when storing the substrates at normal atmosphere.

**Supraparticle synthesis:** Droplets of 3  $\mu\text{L}$  volume, containing the desired amount of FS and NaCl, were deposited from a micropipette onto the superhydrophobic Cu–Ag surface, enclosed in a thin-layer chromatography (TLC) chamber, that is, a sealed glass container that allowed drying at average humidity of  $(43 \pm 10)\%$  and temperature of 21–25°C and the droplets to be observed visually.

**Determination of anisotropy:** The anisotropy of the dry particles was measured with a Carl Zeiss Jenapol optical microscope with images taken with a USB microscope camera (type: DFK 72AUC02, The Imaging Source) at 1280  $\times$  960 resolution and analyzed with ImageJ<sup>[21]</sup> to obtain the ratio of long to short principal axes lengths (length/width:  $D_l/D_w$ ; see Scheme S1).

Received: August 22, 2013

Published online: November 25, 2013

**Keywords:** anisometric particles · colloids · shape control · silica · supraparticles

- [1] Y. S. Xia, T. D. Nguyen, M. Yang, B. Lee, A. Santos, P. Podsiadlo, Z. Y. Tang, S. C. Glotzer, N. A. Kotov, *Nat. Nanotechnol.* **2011**, *6*, 580–587.
- [2] X. J. Feng, L. Jiang, *Adv. Mater.* **2006**, *18*, 3063–3078.
- [3] F. Li, D. P. Josephson, A. Stein, *Angew. Chem.* **2011**, *123*, 378–409; *Angew. Chem. Int. Ed.* **2011**, *50*, 360–388.
- [4] O. D. Velev, S. Gupta, *Adv. Mater.* **2009**, *21*, 1897–1905.
- [5] a) H. Goesmann, C. Feldmann, *Angew. Chem.* **2010**, *122*, 1402–1437; *Angew. Chem. Int. Ed.* **2010**, *49*, 1362–1395; b) J. F. Galisteo-López, M. Ibisate, R. Sapienza, L. S. Froufe-Pérez, A. Blanco, C. López, *Adv. Mater.* **2011**, *23*, 30–69.
- [6] a) D. R. Rolison, *Science* **2003**, *299*, 1698–1701; b) A. Cho, *Science* **2003**, *299*, 1684–1685.
- [7] a) J. P. Ge, H. Lee, L. He, J. Kim, Z. D. Lu, H. Kim, J. Goebel, S. Kwon, Y. D. Yin, *J. Am. Chem. Soc.* **2009**, *131*, 15687–15694; b) J. Kim, Y. Song, L. He, H. Kim, H. Lee, W. Park, Y. Yin, S. Kwon, *Small* **2011**, *7*, 1163–1168; c) T. Kanai, D. Lee, H. C. Shum, R. K. Shah, D. A. Weitz, *Adv. Mater.* **2010**, *22*, 4998–5002.
- [8] a) N. Vogel, C. K. Weiss, K. Landfester, *Soft Matter* **2012**, *8*, 4044–4061; b) L. Isa, K. Kumar, M. Muller, J. Groh, M. Textor, E. Reimhult, *ACS Nano* **2010**, *4*, 5665–5670.
- [9] a) Z. Y. Xiao, A. J. Wang, J. Perumal, D. P. Kim, *Adv. Funct. Mater.* **2010**, *20*, 1473–1479; b) V. Rastogi, K. P. Velikov, O. D. Velev, *Phys. Chem. Chem. Phys.* **2010**, *12*, 11975–11983.
- [10] a) K. Burkert, T. Neumann, J. J. Wang, U. Jonas, W. Knoll, H. Ottleben, *Langmuir* **2007**, *23*, 3478–3484; b) V. Rastogi, O. D. Velev, *Biomicrofluidics* **2007**, *1*, 014107.
- [11] a) O. D. Velev, A. M. Lenhoff, E. W. Kaler, *Science* **2000**, *287*, 2240–2243; b) V. Rastogi, A. A. Garcia, M. Marquez, O. D. Velev, *Macromol. Rapid Commun.* **2010**, *31*, 190–195.
- [12] a) R. D. Deegan, O. Bakajin, T. F. Dupont, G. Huber, S. R. Nagel, T. A. Witten, *Nature* **1997**, *389*, 827–829; b) T. Still, P. J. Yunker, A. G. Yodh, *Langmuir* **2012**, *28*, 4984–4988.
- [13] a) S. T. Chang, V. N. Paunov, D. N. Petsev, O. D. Velev, *Nat. Mater.* **2007**, *6*, 235–240; b) S. J. Ebbens, J. R. Howse, *Soft Matter* **2010**, *6*, 726–738; c) S. Sengupta, K. K. Dey, H. S. Muddana, T. Tabouillot, M. E. Ibele, P. J. Butler, A. Sen, *J. Am. Chem. Soc.* **2013**, *135*, 1406–1414; d) L. Baraban, S. M. Harazim, S. Sanchez, O. G. Schmidt, *Angew. Chem.* **2013**, *125*, 5662–5666; *Angew. Chem. Int. Ed.* **2013**, *52*, 5552–5556.
- [14] W. H. Chong, L. K. Chin, R. L. S. Tan, H. Wang, A. Q. Liu, H. Chen, *Angew. Chem.* **2013**, *125*, 8732–8735; *Angew. Chem. Int. Ed.* **2013**, *52*, 8570–8573.
- [15] U. Kätzel, M. Vorbau, M. Stintz, T. Gottschalk-Gaudig, H. Barthel, *Part. Part. Syst. Charact.* **2008**, *25*, 19–30.
- [16] C. D. Gu, H. Ren, J. P. Tu, T. Y. Zhang, *Langmuir* **2009**, *25*, 12299–12307.
- [17] R. Riquelme, I. Lira, C. Perez-Lopez, J. A. Rayas, R. Rodriguez-Vera, *J. Phys. D* **2007**, *40*, 2769–2776.
- [18] a) L. Pauchard, C. Allain, *Europhys. Lett.* **2003**, *62*, 897–903; b) T. Kajiyu, E. Nishitani, T. Yamaue, M. Doi, *Phys. Rev. E* **2006**, *73*, 011601; c) J. Paulose, D. R. Nelson, *Soft Matter* **2013**, *9*, 8227–8245.
- [19] V. Rastogi, S. Melle, O. G. Calderon, A. A. Garcia, M. Marquez, O. D. Velev, *Adv. Mater.* **2008**, *20*, 4263–4268.
- [20] a) E. Sowade, J. Hammerschmidt, T. Blaudeck, R. R. Baumann, *Adv. Eng. Mater.* **2012**, *14*, 98–100; b) D. Wang, M. Park, J. Park, J. Moon, *Appl. Phys. Lett.* **2005**, *86*, 241114.
- [21] M. D. Abramoff, P. J. Magalhaes, S. J. Ram, *Biophotonics Int.* **2004**, *11*, 36–42.